www.lajss.org
Latin American Journal of Solids and Structures 4 (2007) 179–202

Numerical inertia and damping coefficients determination of a tube-bundle in incompressible viscous laminar fluid

M.V.G. de Morais[1,3,*], F. Baj[1], R.-J. Gibert[1] and J.-P. Magnaud[2]

[1]DRN/DM2S/SEMT/DYN - CEA Saclay - Bât.607
91191 Gif-sur-Yvette Cedex FRANCE
[2]DEN/DM2S/SFME/LTMF - CEA Saclay - Bzât.469
91191 Gif-sur-Yvette Cedex FRANCE
[3]Laboratoire de Mcanique et Matériaux du Génie Civil
Université de Cergy-Pontoise - 5 mail Gay-Lussac - Neuville sur Oise
95031 Cergy-Pontoise Cedex FRANCE

Abstract

In this paper, we compare the performances of Transpiration and ALE methods. The approach ALE (Arbitrary Lagrangian Eulerian) is a powerful tool to treat coupled problems, more precisely, the approach ALE in finite elements of Donea and Hughes. However, ALE performance for determining fluid-elastic forces at small vibrations amplitudes is still ignored. Transpiration method is a simplified approach for calculation of fluid-elastic forces at relatively small vibrations amplitudes. Based on a first order development of velocity boundary conditions, this method allows the use of a fluid domain fixed in time during a dynamic computation, by avoiding hence the problems due to the mesh distortions.

The methods have been validated with help of analytical solution of a vibrating cylinder immersed in stokes confined fluid medium. We made others analysis of dynamics characteristics in tube-bundle comparing with literature. This methods are implemented in Cast3M a numerical platform of French Nuclear Agency - CEA-Saclay -.

Keywords: fluid structure interaction, tube bundle, ALE and Transpiration formulation, CFD, added mass and damping coefficient

1 Introduction

Many industrial components are made of tube array which vibrate under fluid flow. These vibrations, if they are sufficiently intense, can generate troublesome phenomena on the level of the equipment. In a pressurized water nuclear reactor, the tube vibrations phenomena of a steam generator (GV) is an important problem. Indeed, GV's lifespan is directly dependent to these phenomena. Research is still necessary in order to optimize the operation of power plants and to fulfill the restrictive requirements of safety.

*Corresp. author email: marcus.girao-de-morais@u-cergy.fr Received 24 Jan 2007; In revised form 30 Jun 2007

Tube bundles subjected to flow constitute a fluid-elastic coupling problem which interests particularly the nuclear area. Since 60's, several experimental studies were undertaken on reduced model [15]. In order to determine the coupling fluid-elastic behavior, there are mainly two experimental approaches used today:

- ▷ **direct method** - imposed movement of a tube [29], and
- ▷ **indirect method** - tube bundle excited by turbulence [1, 5].

We should be compared the results produced by these two approaches. But we can compare these results only if the experimental conditions are identical for both, because the fluid-elastic forces depend on the geometry of tube array (P/D and geometric disposition) and the flow characteristics (Reynolds Re, Stokes St, and reduced velocity Vr) [26]. As Caillaud [5] shows, **the different experimental flow conditions of direct and indirect methods imply that the results obtained are not easily comparable**, Table 1.

Methods	Vr	Re	St
direct	2 25	1540 4010	61 2005
indirect	0,5 3,5	8400 53100	16800 15200

Table 1: Experimental ranges of Vr, Re and St by direct and indirect methods [5].

The numerical study finds than its place as a comparison tool. The computational fluid dynamic(CFD) have progressed much these last twenty years, parallel to computers performance. The vibration analysis of cylindric obstacles traversed by monophasic flow, a typical problem of fluid-structure interaction (IFS), was already approached numerically by several authors [18, 26, 30]. The majority of the treated cases concerns high vibratory movements, for example, those of a fraction of diameter of tube ($\geq$ 15% D). However our problem concerns small movements limited to the hundredth of diameter of a tube. The experiment shows that physics problems are not the same one, and numerical problems either [15].

We compare, in this paper, the performances of ALE and Transpiration methods to resolve a problem of a cylinder rod vibrating on immobile fluid medium, *i.e.* a typical problem of fluid-structure interaction. We validate both methods with help of analytical solution of a vibrating cylinder immersed in incompressible confined fluid medium. We made others numerical analysis of the dynamics characteristics of an experimental tube-bundle presented in literature. This methods are implemented in Cast3M a numerical platform of French Nuclear Agency - CEA Saclay -.

2 Physical problem

Many industrial components are composed of tube banks which vibrate under the effect of fluid flow. These vibrations, if they are sufficiently intense, can generate troublesome phenomena, fatigue and wear, on the level of support's devices of tubes. Thus, the vibrations of exchange tubes in steam generators (GV) must be analyzed carefully.

External fluid forces may generate large vibrations amplitudes at tubular structures causing possible dramatic damages in terms of nuclear power plant. This vibrations results from four kinds of fluctuation:

1. random fluctuations generated by turbulence in fluids at large Reynolds numbers;
2. fluctuations induced by structure-flow motion coupling due to fluid-elastic effects;
3. resonance with flow periodicity due to vortex shedding; and
4. possible acoustic excitation.

Fluid-elastics coupling forces, case (**ii**), can affect the dynamics behavior of GVs, and be responsible of possible fluid-elastic instabilities. For industrial concerns, it is necessary to be able to predict these fluid-elastic forces ant heir effects on tube bundle dynamic stability. However, a stage **without flow** (fluid-structure coupling) is necessary in order to improve the numerical modelling control of problem.

2.1 Fluid-structure tube bundle model

Firstly, we are interesting on the study of vibrations of a flexible tube belonging to a square fixed tube bundle subjected to a fluid coupling without flow. This configuration is defined by known geometry and hydraulics parameters describing the system [26].

Geometric parameters characterizing a regular square tube bundle are tube diameters D, tube gap P, and tube length L. From mechanical point of view, the flexible tube motion can be modelled by: tube mass M_s, tube damping C_s, and tube stiffness K_s. Concerning the structural movement in the immobile fluid medium, first mode of vibration is affected by added mass M_a and fluid viscosity damping C_a. The equation of motion becomes:

$$(M_s + M_a)\ddot{\mathbf{s}} + (C_s + C_a)\dot{\mathbf{s}} + K_s\ \mathbf{s} = 0 \tag{1}$$

where, $\omega_{fs}^2 = K_s/(M_s+M_a)$ and $\xi_{fs} = (C_s+C_a)/[2\omega_{fs}(M_s+M_a)]$ are the pulsation and damping coefficients of the tube in immobile fluid. To determine the frequency ω_{fs} and damping ratio ξ_{fs} of a spring-mass system vibrating in fluid environment with or without flow, we can use the least-square procedure presented by Gharib *et al.* [14].

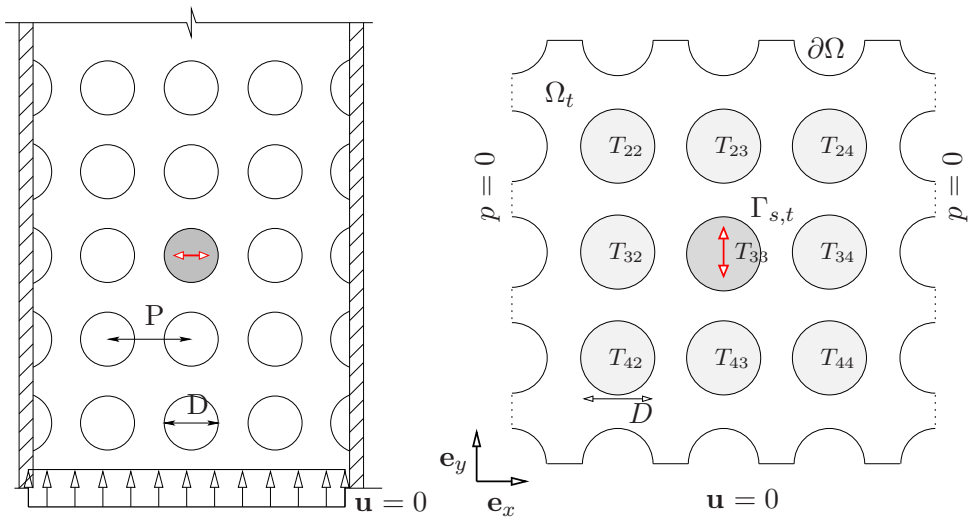

(a) Schematic of AMOVI model (b) Geometry and boundary conditions

Figure 1: Numerical model 2D of tube bundle AMOVI in a fluid at rest.

2.2 Gharib's least square technique

The least squares method can be used to find structural parameters of a mass-spring 1 DOF system subjected to free vibration. Considering a mass-spring system (1) like:

$$a\,\ddot{\mathbf{S}} + b\,\dot{\mathbf{S}} + c\,\mathbf{S} + d\,\mathbf{I} = \mathbf{0} \tag{2}$$

where, $\mathbf{S}$ represent the temporal signal of $\mathbf{s}$ to $[0;t]$. The equation (2) represents a linear equations system redundant with many lines (temporal evolutions $\mathbf{s}^{(i)}$, $i = 0, 1, 2$ taken at each time step) and only four columns. By operating the equation above, we obtain,

$$\left[\dot{\mathbf{S}}\ \mathbf{S}\ \mathbf{I}\right] \left[\begin{array}{c} (b/a) \\ (c/a) \\ (d/a) \end{array}\right] = \left[-\ddot{\mathbf{S}}\right] \tag{3}$$

We multiple equation (3) on each side by $\left[\dot{\mathbf{S}}\ \mathbf{S}\ \mathbf{I}\right]^T$:

$$\left[\begin{array}{ccc} \dot{\mathbf{S}}^T\dot{\mathbf{S}} & \dot{\mathbf{S}}^T\mathbf{S} & \dot{\mathbf{S}}^T\mathbf{I} \\ \mathbf{S}^T\dot{\mathbf{S}} & \mathbf{S}^T\mathbf{S} & \mathbf{S}^T\mathbf{I} \\ \mathbf{I}^T\dot{\mathbf{S}} & \mathbf{I}^T\mathbf{S} & \mathbf{I}^T\mathbf{I} \end{array}\right] \left[\begin{array}{c} (b/a) \\ (c/a) \\ (d/a) \end{array}\right] = - \left[\begin{array}{c} \dot{\mathbf{S}}^T\ddot{\mathbf{S}} \\ \mathbf{S}^T\ddot{\mathbf{S}} \\ \mathbf{I}^T\ddot{\mathbf{S}} \end{array}\right] \tag{4}$$

We can solve this simple system 3×3 by Cramer's rule, for example. The values obtained corresponds to:

$$(c/a) = \frac{K_s}{(M_s + M_a)} \quad \text{et} \quad (b/a) = \frac{(C_s + C_a)}{(M_s + M_a)} \tag{5}$$

or,

$$\boxed{\omega_{fs}^2 = (c/a) \quad \text{et,} \quad 2\omega_{fs}\,\xi_{fs} = \frac{(b/a)}{(c/a)}} \tag{6}$$

The parameter (d/a), that corresponds to force action of mass-spring system, **must be null in case to free vibration**.

2.3 Phase method

Phase method is an other technique to identified de dynamic characteristics of a tube in immobile fluid. At each time step fluid forces acting on the tube are estimated. According to Equation (1), these forces are expressed as function of added mass and viscosity coefficient of damping, $\mathcal{F}_f(t) = -M_a\,\ddot{\mathbf{s}}(t) - C_a\,\dot{\mathbf{s}}(t)$. For an harmonic tube motion $S_o \sin\omega t$, fluid forces $\mathcal{F}_f$ are also periodic:

$$\mathcal{F}_f(t) = \mathcal{F}_o \sin(\omega t + \varphi) \tag{7}$$

where,

$$\mathcal{F}_o = \sqrt{(\omega^2 S_o\, M_a)^2 + (\omega S_o\, C_a)^2} \;\text{ and }\; \tan\varphi = \frac{C_a}{\omega M_a} \tag{8}$$

The in-phase and opposed phase coefficients are given by the expressions:

$$\boxed{\therefore \quad \frac{M_a}{\rho D^2} = \frac{\mathcal{F}_o\,\cos(\varphi)}{\omega^2 S_o} \quad \text{and} \quad \frac{C_a}{\rho\nu} = \frac{1}{\omega_{fs}}\frac{C_a/2\pi St}{\rho D^2} = -\frac{\mathcal{F}_o \sin(\varphi)}{\omega S_o}} \tag{9}$$

where, $2\pi St = \omega_{fs} D^2/\nu$ is the Stokes number. This procedure (9) is very simple to implement: it's necessarily to obtain the values of maximum force $\mathcal{F}_o$ and the phase φ between displacement $\mathbf{s}(t)$ and force $\mathcal{F}_f(t)$. Indeed, the principal disadvantage of this method is that small errors in phase evaluation cause great variations in the determinations of damping C_a to high Stokes number St.

3 ALE formulation

First of all a **system of rectangular cartesian axes** is chosen in which the vectors position ξ, $\mathbf{x}$ and $\mathbf{X}$ will be expressed.

Reference domain Ω_ξ is a $\mathbb{R}^3$ field, Figure 2. An arbitrary movement, described by an application α, deforms this field independently of material particles mouvement. Supposed that α_τ is an homeomorphic geometrical transformation which at every instant τ a point of domain Ω_τ is associated to a point of reference domain Ω_ξ.

$$\begin{aligned} \alpha_\tau : \Omega_\xi &\longrightarrow \Omega_\tau \\ \xi &\longmapsto \mathbf{x} = \alpha(\xi, \tau) \end{aligned} \tag{10}$$

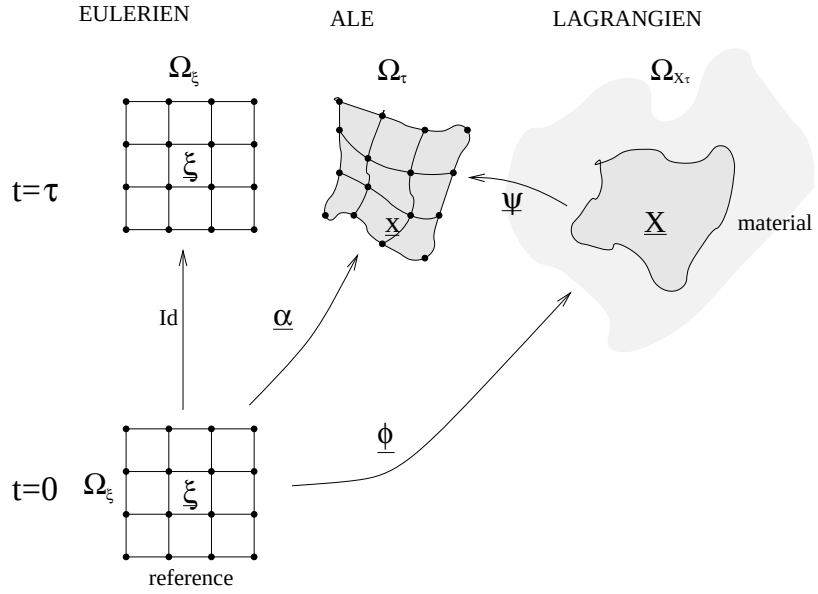

Figure 2: Representation of Eulerian, Lagrangian and arbitraire reference domaines.

We consider that Ω_τ is a $\mathbb{R}^3$ field, Ω_ξ at the moment $t = \tau$, is used as support of grid. The borders movement of this domain is known and regular. The geometrical transformation α_τ is constructed such that it is continuously differentiable bijective mapping ($\mathcal{C}^1$ diffeomorphism class).

Now we consider that the $\Omega_{\mathbf{X}\tau}$ domain, at instant $t = \tau$, contains all material points which were in $\Omega_{\mathbf{X}\xi}$ domain at instant $t = 0$. We define a diffeomorphism ϕ_τ of **material domain** $\Omega_{\mathbf{X}\tau}$ on Ω_ξ domain.

$$\begin{array}{rcl} \phi_\tau : \Omega_{\mathbf{X}\tau} & \longrightarrow & \Omega_\tau \\ \mathbf{X} & \longmapsto & \mathbf{x} = \phi(\mathbf{X}, \tau) \end{array} \tag{11}$$

The relations between the different domaines at $t = \tau$ are indicated on Figure 2. Let define:

$$\boxed{\mathbf{u} = \left.\frac{\partial \phi(\mathbf{X}, t)}{\partial t}\right|_{\mathbf{X}}} \quad \text{and} \quad \boxed{\mathbf{w} = \left.\frac{\partial \alpha(\xi, t)}{\partial t}\right|_{\xi}}. \tag{12}$$

where $\mathbf{u}$ is the velocity of material points and $\mathbf{w}$ is the velocity of reference points. Consequently:

- if the reference volume V_ξ is supposed fixed by choosing $\alpha = Id$, then $\forall\, \tau \quad \Omega_\tau = \Omega_\xi$, $\xi = \mathbf{x}$ and $\mathbf{w} = 0$, *i.e.* **eulerian description**;
- if the reference volume V_ξ follows material volume $V_{\mathbf{X}\tau}$ in its movement, point by point, by choosing $\alpha = \phi$, then $\Omega_\xi = \Omega_{\mathbf{X}\tau}$, $\xi = \mathbf{X}$ and $\mathbf{w} = \mathbf{u}$, *i.e.* **lagrangian description**.

3.1 Fluid domain

The relations obtained in the preceding section make it possible to write the integral form (on spatial domain Ω_t) of the mass and momentum conservation equations on ALE description [16]. We adopted mixed derivative convention $\frac{\delta}{\delta t}$ of Germain [13].

$$\left[\frac{\delta}{\delta t} + (\mathbf{u} - \mathbf{w}) \cdot \nabla\right] \rho(\mathbf{x}, t) = -\rho(\mathbf{x}, t)\, \nabla \cdot \mathbf{u} \tag{13}$$

$$\rho(\mathbf{x}, t) \left(\frac{\delta}{\delta t} + (\mathbf{u} - \mathbf{w}) \cdot \nabla\right) \mathbf{u} = \rho(\mathbf{x}, t)\, \mathbf{b} + \nabla \cdot \overrightarrow{\overrightarrow{\sigma}} \tag{14}$$

The considered fluid is an incompressible newtonian fluid with constant physical properties. Under these conditions, the conservation equations (Navier-Stokes) are written, on a spatial domain Ω_t:

$$\boxed{\begin{cases} \nabla \cdot \mathbf{u} = 0 \\ \dfrac{\delta \mathbf{u}}{\delta t} + (\mathbf{u} - \mathbf{w}) \cdot \nabla \mathbf{u} = -\dfrac{1}{\rho}\, \nabla p + \mathbf{b} + \nu\, \nabla^2 \mathbf{u} \end{cases}} \tag{15}$$

3.2 Solid domain

With small displacements around the configuration of reference, the structural dynamics equations become,

$$M_s \ddot{\mathbf{s}} + C_s \dot{\mathbf{s}} + K_s \mathbf{s} = \mathcal{F}_{f,g} \tag{16}$$

with $\mathcal{F}_{f,g} = \int_{\Gamma_t} \overrightarrow{\overrightarrow{\sigma}} \cdot \mathbf{n}\, ds = \int_{\Gamma_t} [-p \cdot \mathbf{I} + \mu\, \overrightarrow{\overrightarrow{\tau}}] \cdot \mathbf{n}\, ds$ vector of generalized fluid forces.

3.3 Coupled domain

The coupling between solid and fluid equations is operated by boundary conditions on the interface $\Gamma_{s,t}$:

(a) the kinematic continuity velocity,

$$\mathbf{u} = \dot{\mathbf{s}} \qquad \text{(fluid viscous)}; \tag{17}$$

(b) the kinematic continuity of force,

$$\overrightarrow{\overrightarrow{\sigma}} \cdot \mathbf{n} = \overrightarrow{\overrightarrow{\sigma}}_s \cdot \mathbf{n}. \tag{18}$$

Using the equations (15) and (16) with the above boundary conditions, the coupled problem is formulated as follows:

$$\begin{aligned}
\frac{\delta \mathbf{u}}{\delta t} + (\mathbf{u}-\mathbf{w})\cdot\nabla\mathbf{u} - \nu\nabla^2\mathbf{u} &= -\nabla p/\rho + \mathbf{b} \\
\nabla\cdot\mathbf{u} &= 0 \qquad\qquad , \text{in } \Omega_t \\
\mathbf{u} &= \mathbf{u}_\Gamma \qquad\qquad , \text{on } \partial\Omega - \Gamma_{s,t} \\
\mathbf{u} &= \dot{\mathbf{s}} \qquad\qquad , \text{on } \Gamma_{s,t} \\
M_s\,\ddot{\mathbf{s}} + C_s\,\dot{\mathbf{s}} + K_s\,\mathbf{s} &= \\
&= \int_{\Gamma_{f,t}} \left[-p\,\mathbf{n} + \vec{\vec{\tau}}\cdot\mathbf{n}\right]\cdot\varphi_i\,ds \\
(\mathbf{u},\mathbf{s},\dot{\mathbf{s}})|_{\,t=0} &= \left(\mathbf{u}^0,\mathbf{s}^{(0)},\mathbf{s}^{(1)}\right)
\end{aligned} \tag{19}$$

4 Transpiration method

We consider a kind of fluid-structure interaction problems characterized by small structural vibrations around the reference position. The formalism ALE has the disadvantages of appearing an excessive formulation for solving a problem of small vibration like the fluid-elastic coupling in tube bundles.

Thus, before even the advent of the ALE formulation, aeronautics engineers developed a simplified technique, said method of Transpiration [19,26,30]. Based on a first order development of velocity boundary conditions, this method allows the use of a fluid domain fixed in time, by avoiding hence the problems due to the mesh distortions and great adaptations of the fluid solvers. This technique allows simulate vibratory problems of fluid-structure interaction making use of the well-known, reliable and optimized euleriens methods with transpiration boundary conditions [26].

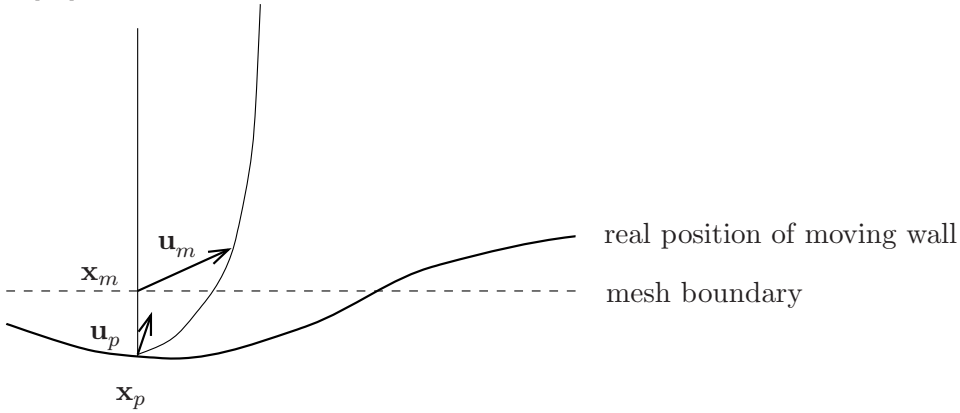

Figure 3: Development of velocity field at structure boundary

Let us suppose a sensible linear velocity field near moving walls. For notations, the index m, p, and o will correspond respectively to the fields (speed, pressure...) evaluated in limit of grid, at moving wall, and stationary position without disturbance of the wall. By definition,

$$\mathbf{x}_p = \mathbf{x}_m + \mathbf{s} \tag{20}$$

The Taylor development of fluid velocity field at interface give,

$$\mathbf{u}_p = \mathbf{u}_m + \mathbf{s} \cdot (\nabla \mathbf{u})_m \,, \qquad \text{in } \Gamma_{s,m} \tag{21}$$

Let us suppose the interface fluid-structure $\Gamma_{s,o}$ be enough regular, the gradient $(\nabla \mathbf{u})_m$ could be approximate to the gradient $(\nabla \mathbf{u})_o$ of steady velocity field $\mathbf{u}^o$ in configuration non-deformed. Thus, the transpiration boundary condition (21) becomes:

$$\mathbf{u}_m = \dot{\mathbf{s}} - \mathbf{s} \cdot (\nabla \mathbf{u})_o \,, \qquad \text{dans } \Gamma_{s,o} \tag{22}$$

where, $\mathbf{u}_p = \dot{\mathbf{s}}$ by adherence conditions.

The forces determination on the structure remains a delicate point. Renou [26] overcome this difficulty by another first order development of stress constraint fields at moving wall, similar to expression (22):

$$\overrightarrow{\overrightarrow{\sigma}} \, (\mathbf{I} + \delta \mathbf{X}) = \overrightarrow{\overrightarrow{\sigma}} + \mathbf{s} \cdot (\nabla \overrightarrow{\overrightarrow{\sigma}})_o, \qquad \text{in } \Gamma_{s,o} \tag{23}$$

4.1 Transpiration coupled domain

The solid and fluid coupling is similar to ALE formulation (19):

$$\begin{aligned}
\frac{\partial \mathbf{u}}{\partial t} + \mathbf{u} \cdot \nabla \mathbf{u} - \nu \nabla^2 \mathbf{u} &= \nabla p / \rho_f \\
\nabla \cdot \mathbf{u} &= 0, && \text{in } \Omega_o \\
\mathbf{u} &= \mathbf{0}, && \text{on } \partial\Omega - \Gamma_{s,o} \\
\mathbf{u} &= \mathbf{s} - \nabla_o \mathbf{u}_o \, \delta \mathbf{x}, && \text{on } \Gamma_{s,o} \\
M_s \, \ddot{\mathbf{s}} + C_s \, \dot{\mathbf{s}} + K_s \, \mathbf{s} &= \\
&= \int_{\Gamma_{s,o}} \left[\overrightarrow{\overrightarrow{\sigma}} + \mathbf{s} \cdot \left(\nabla \overrightarrow{\overrightarrow{\sigma}} \right)_o \right] \cdot \mathbf{n}_o \cdot \varphi_i \, \mathbf{ds}_o \\
(\mathbf{u}, \mathbf{s}, \dot{\mathbf{s}})|_{\,t=0} &= \left(\mathbf{u}^0, \mathbf{s}^{(0)}, \mathbf{s}^{(1)} \right)
\end{aligned} \tag{24}$$

5 Numerical implementation

Now we shut briefly an overview of the numerical implementation of fluid-elastic coupling algorithm. Industrial applications often choose a kind of algorithms known as **partitioned** which

integrate step-by-step each fluid and solid domain independently. The present implementation is strongly inspired by the coupling **improved serial staggered** procedure (**ISS**) [9,24].

An **explicit** staggered partitioned algorithm treat the coupling's conditions, Equations (17) and (18), and geometry Ω_{n+1}, by an explicit approach. Several improvements are made to standard staggered scheme [9,11,12,21–25], that we will discuss.

GCL's condition (*Geometric Conservation Law*), known by Thomas and Lombard works [11,20], shows that temporal variation of each control volume (of time step t^n to t^{n+1}) must be equal to displacement border of cell during time step $\Delta t = t^{n+1} - t^n$. The principal implication of condition GCL is that the grid velocity is an average of the time t^{n+1} and t^n, *i.e.*, $\mathbf{w}^{n+\frac{1}{2}} = (\mathbf{x}^{n+1} - \mathbf{x}^n)/\Delta t$.

Farhat and Lesoinne [11] explain that an explicit staggered procedure built with a fluid solver observing GCL condition didn't respect velocity continuity at interface (17). Consequently, a new asynchronous staggered procedure (**ISS** - Figure 4) was proposed a temporal resolution of solid dynamics by trapezoid rule.

$$\dot{\mathbf{x}}^n \equiv \frac{\mathbf{x}^{n+\frac{1}{2}} - \mathbf{x}^{n-\frac{1}{2}}}{\Delta t} = \frac{\mathbf{s}^n - \mathbf{s}^{n-1}}{\Delta t} + \frac{\dot{\mathbf{s}}^n - \dot{\mathbf{s}}^{n-1}}{2} \equiv \dot{\mathbf{s}}^n,$$

In this way, neither velocity continuity nor GCL condition are violated.

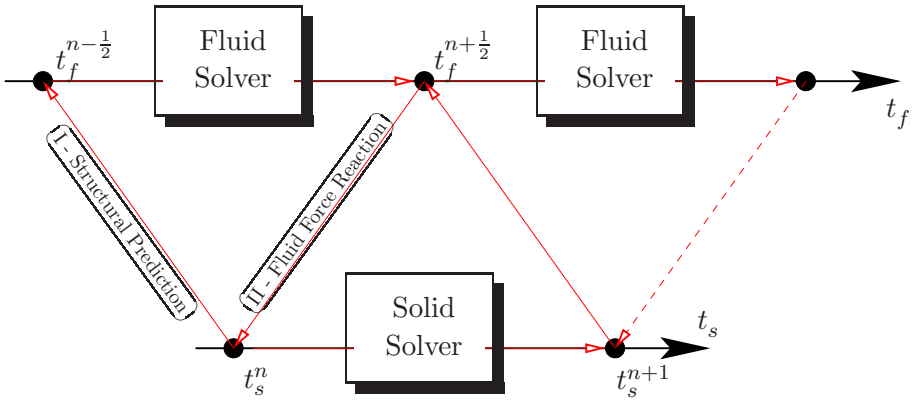

Figure 4: Scheme of improved serial staggered procedure - ISS

For each time step $n+1$, we should solve this coupled system:

$$\left\{ \begin{array}{rcl} (\mathbf{v}^{n+\frac{1}{2}}, p^{n+\frac{1}{2}}) & = & \mathbf{NS}\left(\mathbf{v}^{n-\frac{1}{2}}, \mathbf{w}^{n-\frac{1}{2}}, \mathbf{x}^n, \mathbf{x}^{n+1}\right) \\ (\mathbf{s}^{n+1}, \dot{\mathbf{s}}^{n+1}) & = & \mathbf{MR}\left(\mathbf{s}^n, \dot{\mathbf{s}}^n, \ddot{\mathbf{s}}^n, \mathcal{F}_f^{n+\frac{1}{2}}, \mathcal{F}_s^n\right) \\ \mathbf{x}^{n+\frac{1}{2}} & = & \mathbf{VM}\left(\mathbf{s}^n, \dot{\mathbf{s}}^n, \mathbf{x}^{n-\frac{1}{2}}\right) \end{array} \right. \tag{25}$$

where, **NS** is the projection algorithm for Navier-Stokes resolution, **VM** is an algorithm to determinate mesh velocity $\mathbf{w}$, and **MR** is Newmark time-integration to solve spring-mass model $(\mathbf{s}^{n+1}, \dot{\mathbf{s}}^{n+1})$. For more details, see Morais [8].

5.1 Dynamic mesh algorithm

The transformation of a grid t^{n-1} to t^n controlled by a geometric transformation (dynamic mesh problem) [7,17] is a crucial problem. The difficulty of ALE formulation is to choose arbitrarily a mesh velocity field $\mathbf{w}$ or a node displacement field $\mathbf{x}$ in order to avoid grid degeneration. There are many techniques to solve this problem.

Farhat *et al.* techniques [10] consists to solve the grid displacement like to a fictitious elastic problem.

$$\begin{cases} \bar{\bar{M}}\ \ddot{\mathbf{x}} + \bar{\bar{C}}\ \dot{\mathbf{x}} + \bar{\bar{K}}\ \mathbf{x} = 0, & , \text{in } \Omega_t \\ \mathbf{x}(t) = \mathbf{s}(t) & , \text{on } \Gamma_s \end{cases} \tag{26}$$

where, $\bar{\bar{m}}$, $\bar{\bar{c}}$, $\bar{\bar{k}}$ are arbitrary mass, damping and stiffness terms. Others authors adopts the solution of laplacian equation [4,16] which can be interpreted as a membrane displacement.

We propose here another dynamic mesh algorithm. Indeed, if we deform a convex border by a unit amplitude starting from origin, the subtraction between nodes coordinates of unitary displacement grid $\mathbf{x}\,(\Omega_o)$ and reference grid $\mathbf{x}\,(\Omega_\xi)$ gives a unitary mesh deformation field, Figure 5,

$$\underline{X}_o = \mathbf{x}\,(\,\Omega_o) - \mathbf{x}\,(\,\Omega_\xi)\,.$$

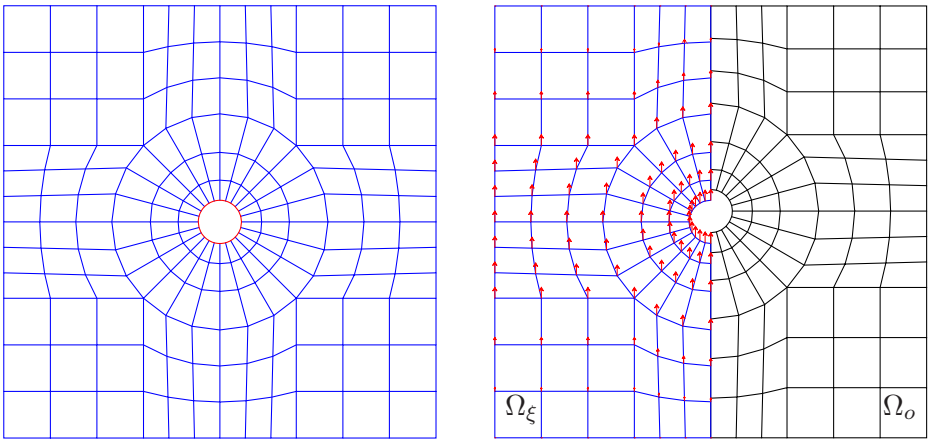

(a) Reference grid Ω_ξ (b) Deformation vector field $\bar{\mathbf{x}}$

Figure 5: Present dynamic mesh technique.

The grid position at time $n+1$ is thus obtained by the expression,

$$\mathbf{x}^{n+\frac{1}{2}} = \mathbf{x}^{n-\frac{1}{2}} + \underline{X}_o \left(\mathbf{s}^n + \frac{\Delta t}{2} \dot{\mathbf{s}}^n \right) \quad \text{et} \quad \mathbf{w}^n = \frac{\mathbf{x}^{n+\frac{1}{2}} - \mathbf{x}^{n-\frac{1}{2}}}{\Delta t}$$

We obtain the expressions of $\mathbf{x}^{n+\frac{1}{2}}$ and $\mathbf{w}^n$ according to two last equations, which one writes formally:

$$\mathbf{x}^{n+\frac{1}{2}} = \mathbf{VM}\left(\mathbf{s}^{n+\frac{1}{2}}, \mathbf{x}^{n-\frac{1}{2}}\right) = \mathbf{VM}\left(\mathbf{s}^n, \dot{\mathbf{s}}^n, \mathbf{x}^{n-\frac{1}{2}}\right)$$

6 Numerical results

6.1 Free vibration of a tube in immobile fluid

We consider a tube of diameter D immersed in an infinite incompressible viscous fluid domain. This tube is excited to an amplitude S_o and then the excitation is removed. We observed the tube vibrations decays in time.

Simulations are made for a tube of diameter $D = 13.30mm$. the amplitude of releasing is limited to $2S_o/D = 0.001$. The experimental tests give frequency $f_{fs,exp.} = 12.866$Hz and ratio damping $\xi_{fs,exp.} = 1.00\%$. The monophasic fluid domain - water - have density $\rho = 1000kg/m^3$, kinematic viscosity $\nu = 10^{-6}m^2/s$ and Stokes number $St \backsimeq 2274$. The coarse mesh ($raf = 0$) is composed by two cylinder concentric of diameters D and $De = 30D$. Total number of elements is $N_r \times N_\theta = 22 \times 48$, where N_r and N_θ is the numbers of nodes in radial and orthoradial directions. Grid refinements ($raf = 1$ and 2) were made dividing each elements into four, encase grid, Figure 6.

Frequency and damping ratio identification of the displacement signal is made by the Gharib's least-square method. Numerical test carry out four periods of simulation of which the first is discarded of analysis.

Time convergence of frequency f_{fs} and damping ratio ξ_{fs} of each method is presented by Figure 7. The numerical results converge towards tests experimental. Transpiration method overestimates the value of added mass. Contrarily, ALE method underestimates it, Figure 7a. Numerical simulations are very close to the analytical solution [6] and experimental tests. The numerical error doesn't exceed $\simeq 0.2\%$.

From the point of view of damping ratio, Figure 7b, the time convergence observes a similar behavior of frequency. ALE method converge more quickly than Transpiration method. The better numerical performance of ALE formulation is due to the exact description of moving wall.

Figure 8 presents the evolution of relative error compared to experimental test. We find a behavior in power law $\phi_{ref} = \phi_6 - C\ N^{\alpha_t}$ according to Richardson hypothesis [28]. The convergence order α_t of ALE and Transpiration method are close to unit ($\alpha_t \simeq 1$), in conformity with the theoretical slope of our coupling algorithm.

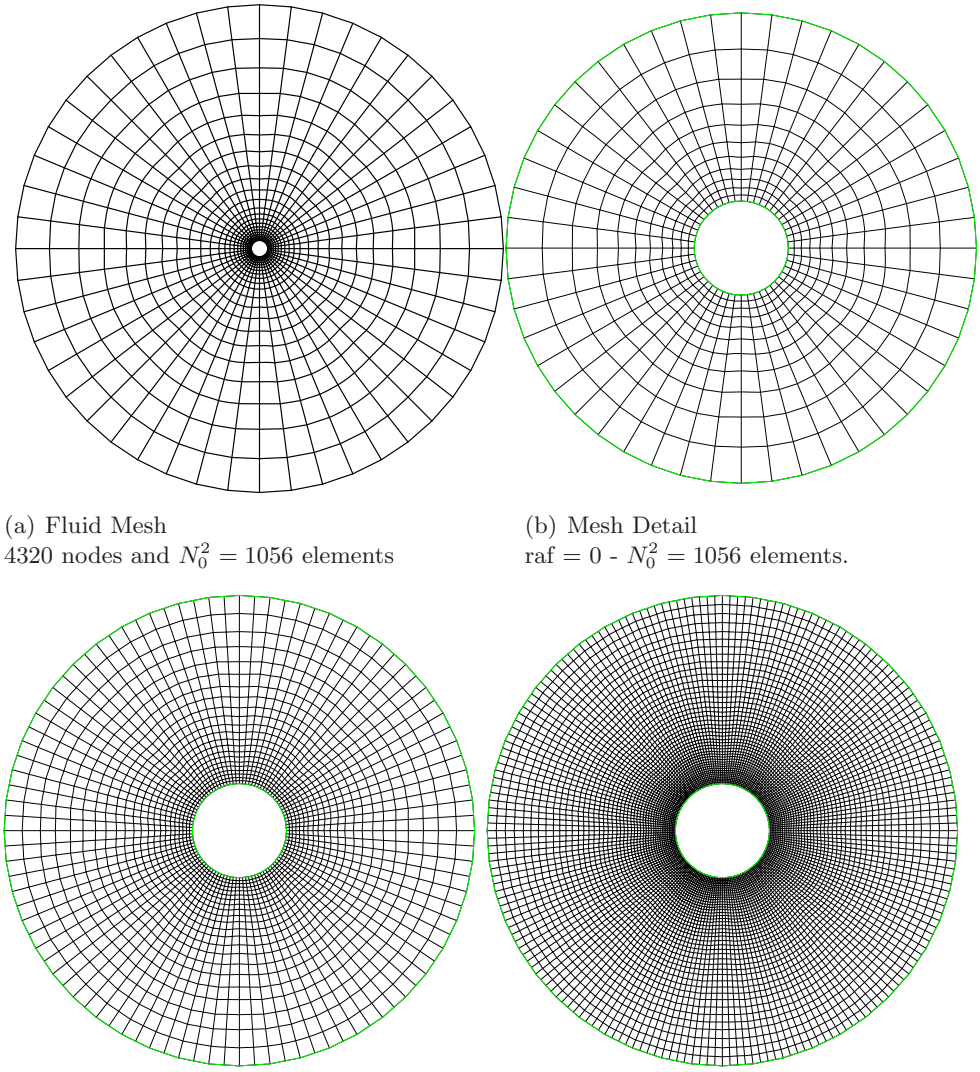

(a) Fluid Mesh
4320 nodes and $N_0^2 = 1056$ elements

(b) Mesh Detail
raf = 0 - $N_0^2 = 1056$ elements.

(c) Mesh Detail
raf = 1 - $N_1^2 = 4224$ elements.

(d) Mesh Detail
raf = 2 - $N_2^2 = 16896$ elements.

Figure 6: Original fluid mesh (a) and zoom details of encase fluid mesh (5 radiis from origins).

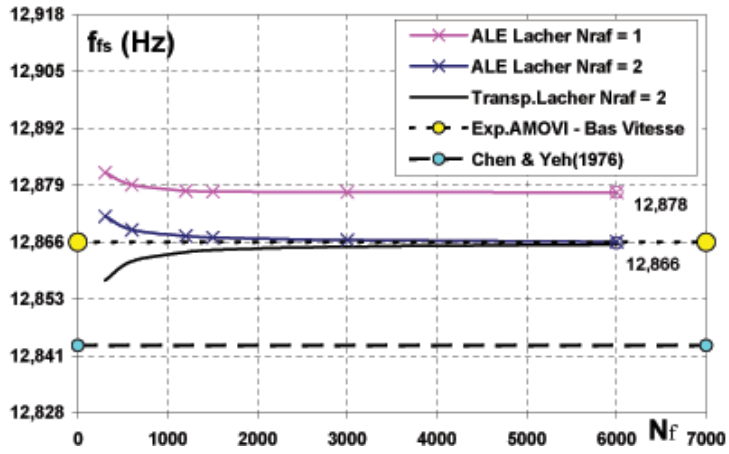

(a)

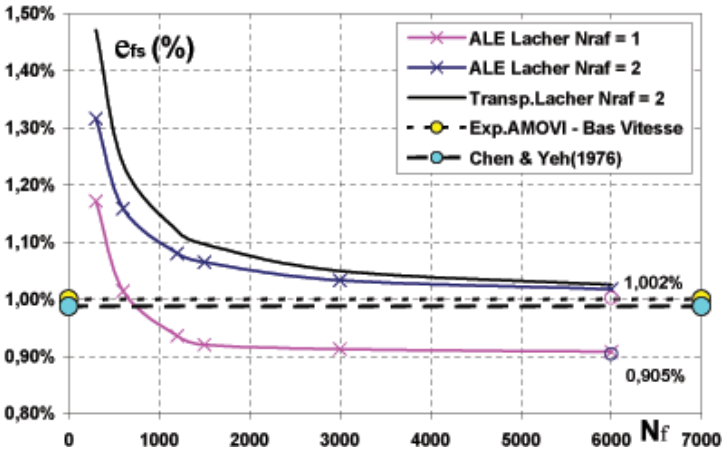

(b)

Figure 7: ALE and Transpiration time convergence of tubes + fluid system.

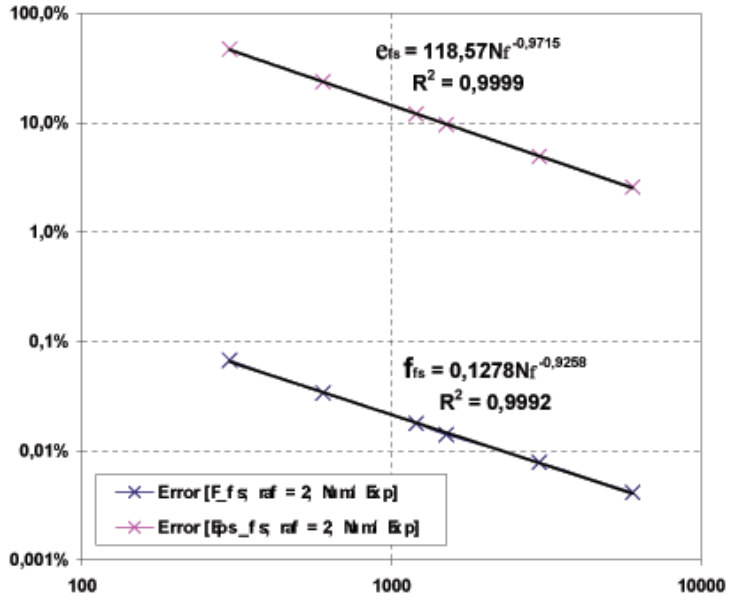

(a) Transpiration

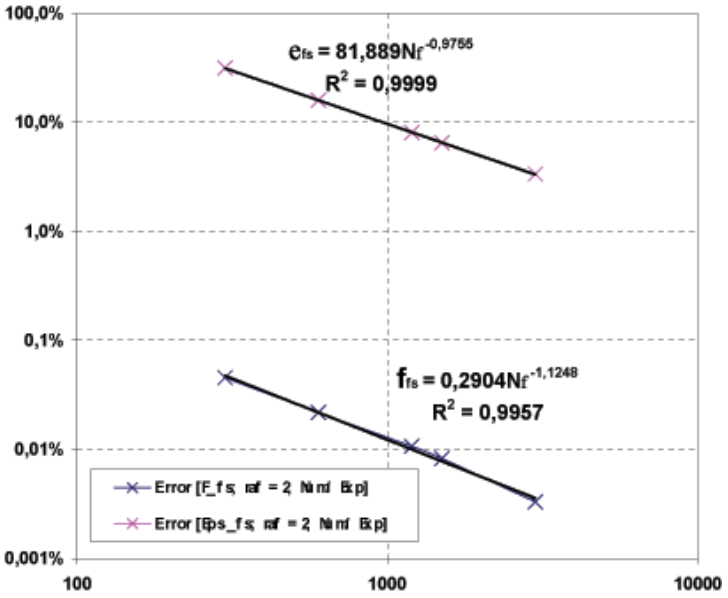

(b) ALE

Figure 8: Relative error of frequency and damping ratio of coupled system.

According to Richardson extrapolation [28], the converged value ϕ_{ref} is obtained by the expression: $\phi_{ref} = \phi_{N_\varphi/2} + [\phi_{N_\varphi/2} - \phi_{N_\varphi}]/[1 - 2^{\alpha_t}]$, where α_t is the time convergence order, N_φ and $N_\varphi/2$ are respectively the numerical results with $2\pi/N_\varphi$ and $4\pi/N_\varphi$ time steps ($\omega\Delta t = 2\pi/N_\varphi$). Knowing that the time convergence order of the present coupling algorithm is linear ($\alpha_t \simeq 1$), the expression of ϕ_{ref} become:

$$\phi_{ref,t} = 2\phi_{N_\varphi/2} + \phi_{N_\varphi} \tag{27}$$

Table 2 synthesizes converged results by Richardson extrapolation comparing with experimental and analytical values.

	ALE		Transpiration		AMOVI	Chen&Yeh
	$raf = 1$	$raf = 2$	$raf = 1$	$raf = 2$		
f_{fs}(Hz)	12,878	12,866	12,876	12,866	12,87	12,84
ξ_{fs}(%)	0,905	1,002	0,858	1,002	1,00	0,99

Table 2: Summary of numerical, experimental and analytical results.

6.2 Fluid-structure coupling of AMOVI tube array model

Fluid-structure coupling (vibration in fluid domain without flow) of AMOVI tube array model is modelled in 2D square 9-tube bundle with tube-to-tube spacing $P/D = 1,44$ and diameter $D = 12,15\ mm$, Figure 1. The flexible tube at central tube array has one vibration mode. All other tubes are fixe. In order to avoided boundary effects, two lines of half-tubes at $\mathbf{e_x}$ direction were added around of 9-tube configuration screw to the metal walls. Consequently, the other two lines of tubes at upstream and downstream flow direction ($\mathbf{e_y}$) were also cut out forming a symmetrical unit. Numerical tests showed that the no-slip boundary conditions ($\mathbf{u} = 0$) at walls sides and null pressure ($p = 0$) at upstream and downstream direction obtain same results compared to a entire modelling of AMOVI model.

The monophasic fluid - water - have mass density $\rho = 1000\ kg/m^3$ and kinematic viscosity $\nu = 10^{-6}m^2/s$. The flexible tube belonging to a fixed tube bundle in 9-tube configuration have the following vibratory characteristics in vacuum: circular frequency $\omega_s = 2\pi \cdot 14,30 = 89,85rad/s$, ratio damping $\xi_s = 0.25\%$ and linear density $M_s = 0,298kg/m$. Consequently, stiffness and structure damping constants are respectively $K_s = 2405,7kg/m/s^2$ and $C_s = 0,130kg/m/s$. According to experimental results with low Reynolds flow in AMOVI model [2], the vibratory characteristics under water are circular frequency $\omega_{fs} = 2\pi \cdot 11,90 = 74,76rad/s$ and ratio damping $\xi_{fs} = 1,17\%$. Consequently, Stokes number is $St = 1757$.

The flexible tube shake on $\mathbf{e_y}$ direction with adimensional amplitude $S_o/D = 0,001$. Numerical tests with imposed and free movement were carried out for each formulation in order to verify the results convergence.

6.2.1 Numerical criteria

In order to have the control of numerical modelling, the optimal grid and time-step characteristics for simulations will be treated in this item. First of all, it is necessary to define the **characteristic length** $\delta = \delta'/R$ of boundary layer on the moving walls. For an oscillating cylinder problem in laminar fluid, Figure 9a, the characteristic length can be define as $\delta \leq 1/\sqrt{\pi St/2}$.

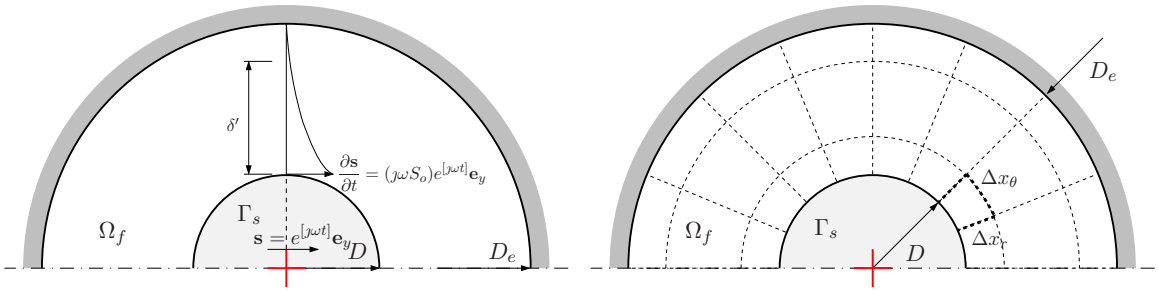

(a) Characteristic length of fluid δ (b) Scheme of space discretization

Figure 9: Vibration of a cylinder rod in incompressible viscous laminar fluid.

Spatial Criteria - The numerical description of the vibratory phenomena in boundary layer is essential for this kind of problem. To insurer a minimum of $\mathcal{C}$ elements in boundary layer, $\delta D/2 \geq \mathcal{C}\Delta x_r$, we develop an elementary spatial criteria. By definition, the finite elements near fluid-structure walls Γ_s are square $\Delta x_r \approx \Delta x_\theta = \pi D_1/N_\delta$, being N_δ the number of nodes around fluid-structure walls Γ_s. We obtain $N_\delta \geq \mathcal{C} \cdot \pi\sqrt{2\pi St}$. Then, an estimation of nodes around the flexible tube is $N_\delta \geq \mathcal{C} \cdot 330$ orthoradial nodes. We use quadratic element Q2-Q1 . Others numerical tests show that a grid with an element in boundary layer limite ($\mathcal{C} = 1$) (40840 elements and 126079 nodes) offer a good precision with a lower-cost computational, Figure 10.

Phase Criteria - The numerical time criteria is also necessary for vibratory phenomena. The numerical analysis of problem [8] shows that the criterion more restrictive is due to signal identification procedure. The error sensitivity analysis of signal identification procedure (9) gives the expressions of error propagation δM_a and δC_a:

$$\frac{\delta M_a}{M_a} \geq \tan(\varphi)\delta\varphi \quad \text{and} \quad \frac{\delta C_a}{C_a} \geq \frac{1}{\tan(\varphi)}\delta\varphi \tag{28}$$

We can estimate an optimal number of time-step per period N_φ ($\Delta\varphi = \omega\Delta t = 2\pi/N_\varphi$) using the analytical solutions of a cylinder rod vibrating in viscous fluid. But, a more correct estimate must take to account confinement effects of close tubes. Using an interpolation technique, Rogers *et al.* [27] finds a relation between confinement ratio D_e/D and pitch-to-diameter ratio P/D, *i.e.*, $D_e/D = [1,07 + 0,56\ P/D] \cdot P/D$. Then, the expressions of added mass M_a and damping coefficient C_a for a cylinder rod immersed in stokes confined fluid medium are given by [6]:

$$\frac{M_a}{\rho D^2} = \frac{\pi}{4}\frac{1+(D/D_e)^2}{1-(D/D_e)^2} \quad \text{and} \quad \frac{1}{\omega}\frac{C_a}{\rho D^2} = \frac{\pi}{\sqrt{\pi St}}\frac{1+(D/D_e)^3}{[1-(D/D_e)^2]^2} \tag{29}$$

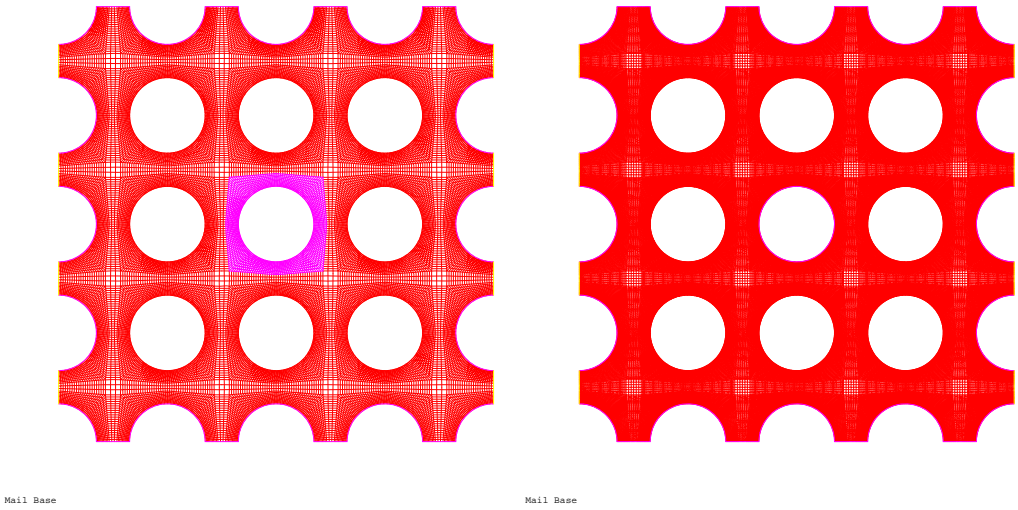

(a) $raf. = 0 - N_\delta = 168$ orthoradial nodes (b) $raf. = 1 - N_\delta = 336$ orthoradial nodes

Figure 10: Encased fluid grids of AMOVI tube array model.

Applicant the expressions (29) and (8b) in the equation of error propagation (28b), one obtains:

$$\frac{N_\varphi}{2\pi} \cdot \frac{\delta C_a}{C_a} \gtrsim \frac{\sqrt{\pi St}}{4} \cdot \frac{\left[1 + (D/D_e)^2\right] \cdot \left[1 - (D/D_e)^2\right]}{1 + (D/D_e)^3} \tag{30}$$

For present problem, the AMOVI tube array model ($P/D = 1,44$) have confinement ratio $D_e/D = 2,702$. One defines the number of time-steps per period $N_\varphi \simeq 2\pi/\delta\varphi$ ($\Delta\varphi \lesssim \delta\varphi$). Thus the optimal number of time-step is $N_\varphi \cdot (\delta C_a/C_a) \geq 109$. For an relative error $\delta C_a/C_a \simeq 1\%$, the phase number N_φ optimal is 10900 time-steps per period .

6.2.2 Numerical results analysis

The comparisons between ALE and of Transpiration methods are carried out under same geometrical and initial conditions. We use Pentium 4 Xeon© 3GHz computers with 2Go of memory to carry out ours simulations on forced movement and free vibration with three and four periods of vibration, respectively. The signal identification procedures are the Phase method for forced movement and the Gharib's least-square method for free vibration. Phase method analyses the last period, while Gharib's method uses the last three periods to find the frequency and damping ratio.

The Figure 11 compares the pressure fields at maximum velocity obtained by ALE and Transpiration. The ALE and Transpiration pressure fields aren't symmetric with the horizontal axis due to the confinement effects of close tubes.

Figure 12 present the frequency f_{fs} and damping ratio ξ_{fs} evolution on function of phase number $N_\varphi \in [300 - 4600]$ for Transpiration and ALE methods. Table 3 summarizes numerical frequency, damping results, and corresponding added mass M_a and damping coefficient C_a,

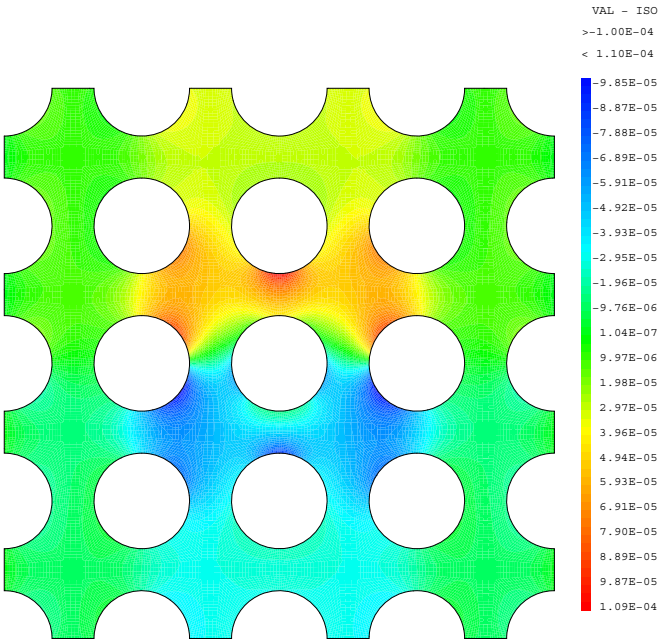

(a) ALE

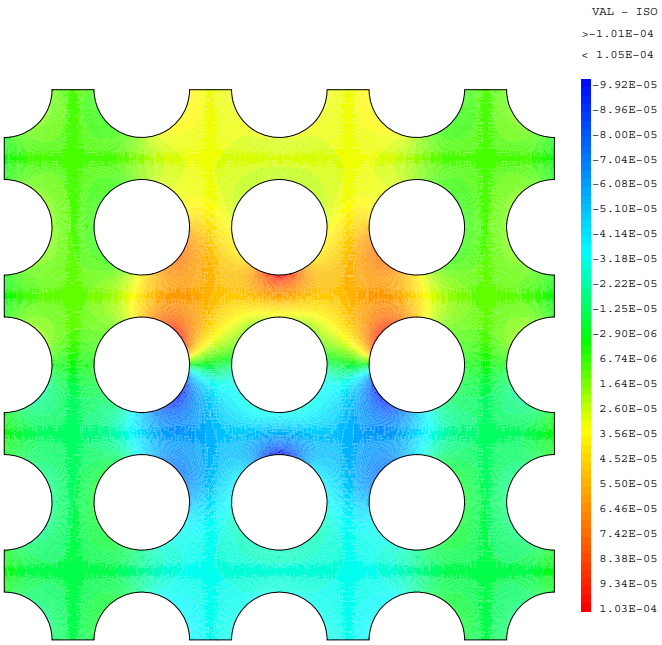

(b) Transpiration

Figure 11: Comparison of pressure fields at maximum velocity.

identified by free vibration and forced movement procedures. This results are compared with Roger's semi-analytical solution, low-Reynods experimental test of AMOVI model, and other numerical results - CREATIVE EdF-CEA co-operative work group [3]-.

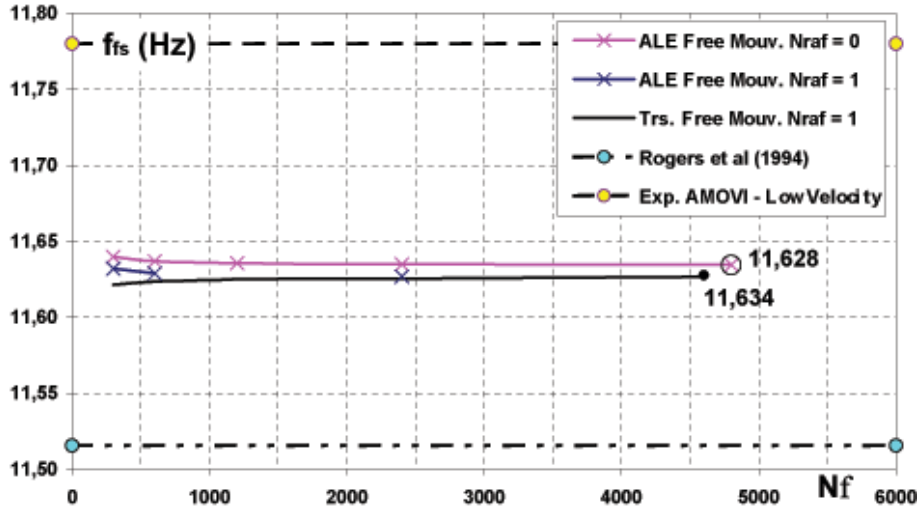

(a) Frequency f_{fs}(Hz)

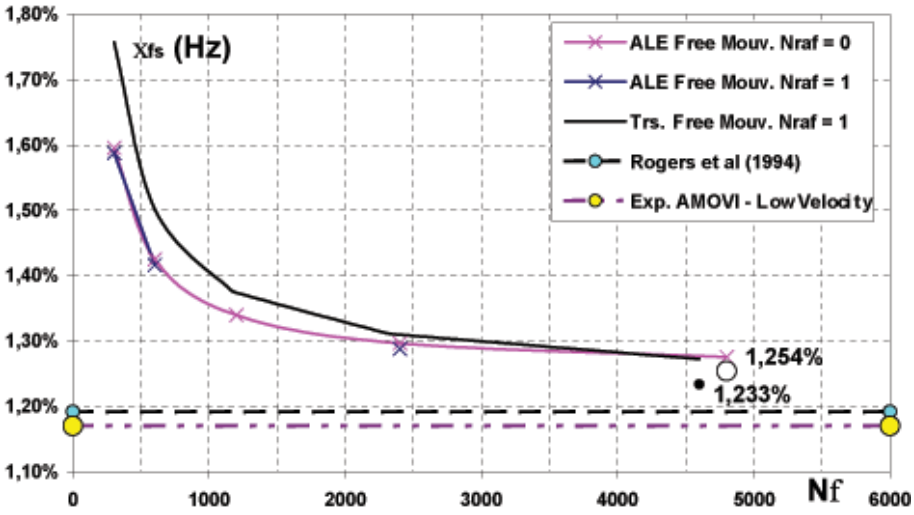

(b) Damping ratio ξ_{fs}(%)

Figure 12: ALE and Transpiration time convergence of tube+fluide system. **OBS:** Each vertical scale subdivisions correspond to a relative error $\delta\varepsilon \simeq 0.4\%$ in frequency and $\delta\varepsilon \simeq 9\%$ in damping.

Table 3 synthesizes converged results by Richardson extrapolation comparing with experimental and analytical values. Time convergence of coupling algorithms have a monotonous asymptotic behavior even with small N_φ.

The ALE and Transpiration differences are only shown for damping ratio evolution that

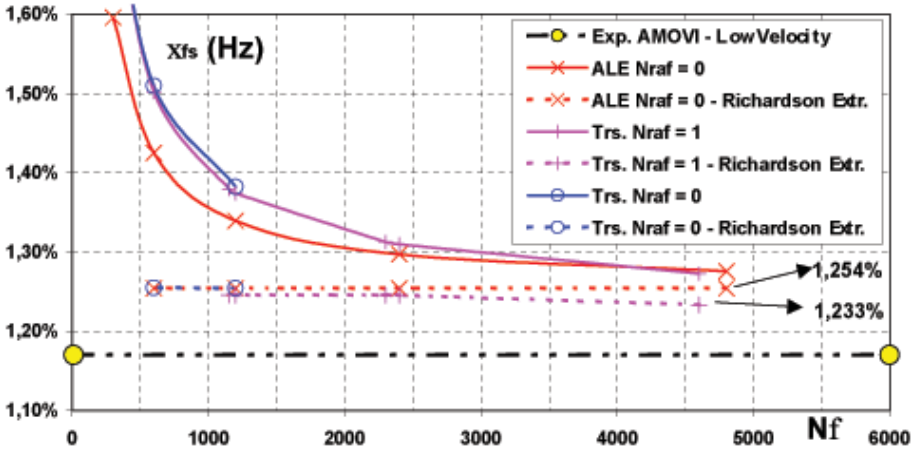

Figure 13: Richardson extrapolation (27) per report time convergence of damping ratio $\xi_{fs}(\%)$ of tube+fluide system.

does not exceeding 2.5% for Transpiration method. The frequency results are similar for both methods. A spatial discretization $N_\delta = 21$ nodes offer alike results then to $N_\delta = 42$ nodes.

	Transpiration		ALE		AMOVI	Rogers	Creatif
	$raf = 0$	$raf = 1$	$raf = 0$	$raf = 1$	Low Re		EdF
Free Vibration							
f_{fs}(Hz)	11,634	11,634	11,626	11,628	11,78	11,55	11,887
$\xi_{fs}(\%)$	1,254	1,210	1,245	1,233	1,17	1,16	1,165
Forced Movement							
M_a	1,0886	1,0359	1,0886	1,0359	0,9561	1,0769	0,9028
C_a	0,06807	0,06404	0,06807	0,06404	0,05736	0,05964	0,05586
f_{fs}(Hz)	11,526	11,625	11,526	11,625	11,78	11,55	11,887
$\xi_{fs}(\%)$	1,321	1,265	1,321	1,265	1,17	1,16	1,165

Table 3: Summary of numerical, experimental and semi-analytical results.

7 Conclusions

In this present work, we carry out a numerical analysis of dynamical characteristics of AMOVI square tube-bundle experimental model. We analyse the numerical performances of ALE and Transpiration methods. We present two examples: (a) free vibration of a tube in viscous laminar fluid, and (b) free vibration and imposed movement of a tube into a rigid 9x9 tube-array.

ALE and Transpiration results of first case have been validated with help of analytical solution and experimental data. We develop numerical criteria to control the results quality.

Finally, to last one, we carry out a numerical dynamical analysis of the experimental mock-up AMOVI composed of a mobile cylinder into a rigid 9x9 tube-array with fluid. We compare the numerical results to experimental data, other numerical results and the semi-analytical solution of Roger *et al.* [27].

ALE and Transpiration implementation show similar converged results. The hypothesis of small vibrations, made by Transpiration method, is valable to fluid-structure problems (without fluid flow). Transpiration method converge a little slower than ALE.

Further developments will be carried out in order to improve the coupling process with flow dynamics and mobile boundaries.

Acknowledgements The first author acknowledges the financial support by a Brazilian CAPES Fellowship, Process No. 1232/99-1.

References

[1] F. Baj. *Amortissement et instabilite fluide-elastique d'un faisceau de tubes sous ecoulement diphasique*. These de doctorat, Universite Paris VI, 1998.

[2] F. Baj. Adimensionnement des forces de couplage fluide-structure : etudes parametriques en monophasique (eau) et en diphasique (eau-air). influence des modeles cinematiques. Rapport d'etudes SEMT/DYN/RT/00-043/A, CEA Saclay - DMT, 2000.

[3] Z. Bendjeddou. *Metodologie pour la simulation numerique des vibrations induites par ecoulement dans les faisceaux de tubes*. These de doctorat, Universite de Lille, 2005.

[4] Z. Bendjeddou, M. Souli, and E. Longatte. Application of arbitrary lagrange euler formulations to flow-induced vibration problems. *J. of Pressure Vessel Technology - Transactions of the ASME*, 125:411–417, 2003.

[5] S. Caillaud. *Excitation forcee et contrle actif pour la mesure des forces fluide-elastiques*. These de doctorat, Universite Pierre et Marie Curie - Paris VI, 1999.

[6] S. S. Chen. *Flow-induced vibration of circular cylindrical structures*. Hemisphere Publ. Corp., Washington, 1987.

[7] C. Conca, J. PLanchard, B. Thomas, and M. Vanninathan. *Problemes mathematiques en couplage fluide-structure - Aplications aux faisceaux tubulaires*, volume 70 of *Collection de la Direction des Etudes et Recherches d'Eletricite de France*. Editions Eyrolles, 1994.

[8] M. V. G. de Morais. *Qualification numrique des mthodes de modlisation des forces fluide-lastiques s'exerant dans un faisceau de tubes en coulement transversale*. These de doctorat, Universite d'Evry val d'Essonne, 2006.

[9] C. Farhat and M. Lesoinne. Improuved staggered algorithms for the serial and parallel solution of three-dimensional non-linear transient aeroelastic problems. Report 97-11, Centre Aerospace Structures - University of Colorado, Boulder, Colorado, 1997. AIAA Journal, 36(9),pp.1774-1757,(1996).

[10] C. Farhat, M. Lesoinne, and N. Maman. Mixed explicit/implicit time integrations of coupled aeroelastic problems: three-field formulation, geometric conservation and distributed solution. *Internation Journal for Numerical Methods in Fluids*, 21(8):807–835, 1995.

[11] M. Lesoinne C. Farhat. Geometric conservation for flow problems with moving boundaries and deformable meshes, and their impact on aeroelastic computations. *Comput. Meths. Appl. Mech. Engrg.*, 134:71–90, 1996.

[12] C.A. Felippa, K.C. Park, and C. Farhat. Partitioned analysis of coupled mechanical systems. *Comput. Meths. Appl. Mech. Engrg.*, 190(24-25):3247–3270, 2001.

[13] P. Germain. *Mecanique*, volume 1. Ellipses Marketing Edition, 1986.

[14] M. R. Gharib, A. Leonard, and M. Gharib. A fluid force deduction technique for vibrating structures in cross-flow. In *Flow-Induced Vibration*, Proceedings of the 7th International Conference on Flow-Induced Vibration - FIV2000 / Lucerne / Switzerland, pages 85–89, 2000.

[15] R.-J. Gibert. *Vibrations des Structures - Interactions avec les fluides - Sources d'excitation aleatoires*, volume **69** of *Collection de la Direction des Etudes et Recherches d'Eletricite de France - CEA-EDF-INRIA Ecole d'ete d'analyse numerique*. Editions Eyrolles, 1988.

[16] S. Gounand. Simulation numerique d'ecoulements a surface libre. Technical report, CEA/Saclay - DRN/DMT/SEMT/TTMF, 1997.

[17] N. Greffet. *Simulation couplee fluide-structure appliquee aux problemes d'instabilite non-lineaire sous ecoulement*. These de doctorat, L'ecole Normale Superieure de Cachan, 2001.

[18] A. Huerta and W. K. Liu. Viscous flow structure interaction. *Journal of Pressure Vessel Technology*, 110:15–21, 1988.

[19] M.J. Lighthill. On displacement thickness. *J. Fluid Mechanics*, 4:383–392, 1958.

[20] B. Nkonga and H. Guillard. Godunov type method on non-structured meshes for three-dimensional moving boundary problems. Rapport de Recherche N 1883, INRIA, 1993.

[21] S. Piperno. *Simulation numerique des phenomenes d'interation fluide-structure*. These de doctorat, ecole Nationale de Ponts et Chaussees, 1995.

[22] S. Piperno. Explicit/implicit fluid/structure staggered procedures with a structural predictor and fluid subcycling for 2D inviscid aeroelastic simulations. *Int. J. Numer. Meth. Fluids*, 25:1207–1226, 1997.

[23] S. Piperno and C. Farhat. Design and evaluation of staggered partitioned procedures for fluid-structure interactions simulations. Rapport de Recherche 3241, INRIA, Unite de Recherche Sophia-Antipolis, France, 1997.

[24] S. Piperno and C. Farhat. Partitioned procedures for transient solution of coupled aeroelastic problems - part ii: Energy transfer analysis and three-dimensional applications. *Comput. Methods Appls. Mech. Engrg.*, 190:3147–3170, 2001.

[25] S. Piperno, C. Farhat, and B. Larrouturou. Partitioned procedures for transient solution of coupled aeroelastic problems - part i: Model problem, theory and two-dimensional application. *Comput. Methods Appls. Mech. Engrg.*, 124:79–112, 1995.

[26] J.-Y. Renou. *Une methode eulerienne pour le calcul numerique de forces fluides-elastiques*. These de doctorat, Universite Paris VI - Pierre et Marie Curie, 1998.

[27] R. J. Rogers, C. Taylor, and M. J. Pettigrew. Two-phase flow-induced vibration : an overview. *Journal of Pressure and Vessel Technology - Transactions of the ASME*, 116:233–253, 1994.

[28] C. J. Roy. Review of code and solution verification procedures for computational simulation. *Journal of Computational Physics*, 205:131156, 2005.

[29] H. Tanaka, K. Tanaka, and F. Shimizu. Characteristics of tube bundle vibrations in cross flow. In S. Ziada & T. Staubli, editor, *Flow Induced Vibrations - Proceedings of the 7th International Conference on Flow-Induced Vibration - FIV2000*, pages 473–480. A.A. BALKEMA, 2000.

[30] M.A. Fernandez Varella. *Modeles simplifies d'Interaction Fluide-Structure*. These de doctorat, Universite Paris IX Dauphine, 2001.